ACS OMEGA

http://pubs.acs.org/journal/acsodf

Article

Stability Evaluation of Aflatoxin B_1 Solution Certified Reference Material *via* Ultra-High Performance Liquid Chromatography Coupled with High-Resolution Mass Spectrometry

Shuangqing Li, Xiaomin Li,* Xuehui Liu, Qinghe Zhang, Jiaqi Fang, Xiuqin Li, and Xiong Yin*

Cite This: *ACS Omega* 2022, 7, 40548−40557

Read Online

ACCESS | Metrics & More | Article Recommendations | Supporting Information

ABSTRACT: Aflatoxin B_1 (AFB_1) solution certified reference materials (CRMs) have been widely utilized in the measurements of AFB_1 contaminations in foods and agricultural products. It is of great importance to evaluate the stability of AFB_1 solution CRMs in different matrices for their practical applications. In this study, the stability of AFB_1 solution CRM was investigated and its degradation products under various conditions were elucidated using ultra-high performance liquid chromatography coupled with high-resolution mass spectrometry for the first time. Exposure to high temperatures and UV light irradiation accelerated the degradation of AFB_1 solution significantly, and the degradation products were largely dependent on the solvents. Two degradation pathways were proposed based on the degradation products. The addition reaction, oxidation reaction, and modification of the methoxy group are the major processes involved in the degradation of the AFB_1 solution. The results of this study indicate that the property value of the acetonitrile solution of AFB_1 can be well retained when it is stored at temperatures lower than 60 °C, and the exposure to UV light irradiation is avoided.

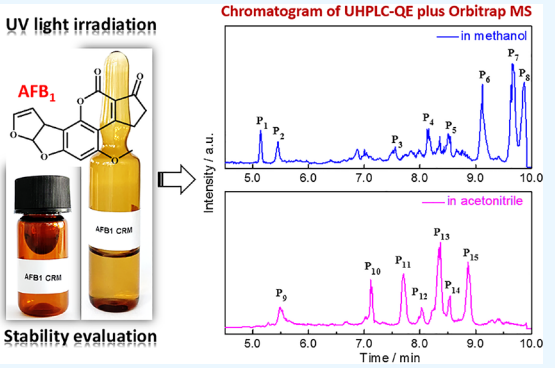

1. INTRODUCTION

Aflatoxins are low-molecular-weight secondary metabolites produced mainly by the fungal species *Aspergillus flavus*, *Aspergillus parasiticus*, and *Aspergillus nomius*.[1−3] Up to now, about 20 different types of aflatoxins have been found in nature.[4] As one of the aflatoxins, aflatoxin B_1 (AFB_1, its chemical structure shown in Figure 1) has been classified as a group I carcinogen by the International Agency Research on Cancer (IARC).[5] It has been widely found in agricultural commodities and foods, i.e., grains, vegetables, oils, milk, and eggs.[6−9] In addition, AFB_1 is highly toxic and has been identified as hepatotoxic, carcinogenic, and teratogenic and can cause other specific symptoms.[3,10] Thus, AFB_1 is the subject of the regulations on foods and agricultural feeds. The corresponding legislation in over 80 countries has established the maximum permitted limit of AFB_1 in various foods and agricultural commodities aiming to protect human beings and animals.[10−12] Accurate measurement of AFB_1 in various matrices is a prerequisite for effectively limiting the fractions of AFB_1 in agricultural products and foods. The method has been developed to measure the fraction of AFB_1 in solutions fast and facilely using ultra-high performance liquid chromatography (UHPLC) coupled with a diode array detector (DAD) or mass spectrometry (MS). It has been considered the golden approach for the measurement of AFB_1 fractions due to its high reproducibility and accuracy.[8,13−16] Nevertheless, the accuracy of this method largely relies on the certified reference materials (CRMs) of AFB_1 solutions prepared with various organic solvents.

CRMs are widely used for quality control, calibration of instruments, and validation of analytical methods.[17−19] To the best of our knowledge, the CRMs of the AFB_1 solution have been rarely reported. This is possibly due to the high toxicity and limited stability of AFB_1 in solutions. The National Institute of Metrology, China (NIM) has launched an international comparison of the AFB_1 CRM in coordination with the Bureau International des Poids et Mesures (BIPM) in 2019.[20−23] The comparison was conducted in cooperation with 10 countries from Africa, America, Asia, and Europe.[20] It was found that the property value of the sample, which is the acetonitrile solution of AFB_1, remained stable in the international comparison when the sample was shipped and stored in the dark and at controlled temperatures.[20] However, studies also revealed that the solvent of the AFB_1 solution, the ambient temperature, and the exposure to light might have a great effect

Received: September 8, 2022
Accepted: October 12, 2022
Published: October 24, 2022

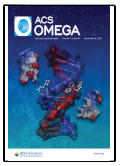

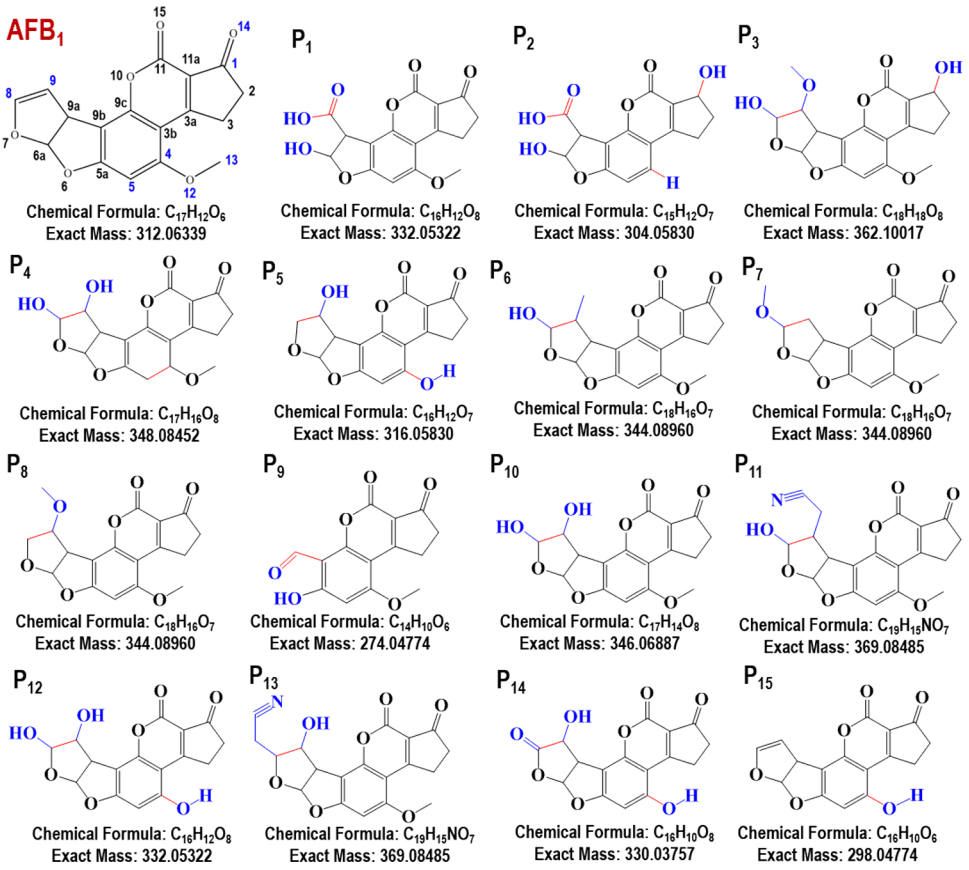

Figure 1. Chemical structure of aflatoxin B_1 (AFB_1) and proposed chemical structures of its degradation products (P_1 to P_{15}) produced by UV light exposure treatment in methanol and acetonitrile.

on the stability of the solution CRMs. Therefore, it is crucial for the preparation, distribution, storage, and application of AFB_1 solution CRMs to investigate the stability of AFB_1 solution under various conditions. The stability of AFB_1 in a few types of matrices has been investigated, and the degradation pathways of AFB_1 were studied upon the decontamination or detoxification treatments, including electrolyzed oxidizing, ozonolysis, and exposure to γ-ray, electron beam, or high-voltage atmospheric cold plasma.[4,24−30] Previous studies also indicated that the aflatoxins tended to degrade in aqueous solution or in the solvents containing water when stored at 4 or 20 °C.[31−35] Nevertheless, the stability of the AFB_1 solution CRMs has not been systematically studied, and the degradation mechanism of the AFB_1 solution CRMs has not been fully understood, although such knowledge is essential for the development and utilization of the AFB_1 solution CRMs.

In this study, the stability of AFB_1 solutions was evaluated, and the related degradation mechanisms were investigated by using UHPLC coupled with high-resolution Q Exactive plus Orbitrap mass spectrometry (QE plus Orbitrap MS) aiming at further advancing the application of the AFB_1 solution CRMs. The effects of different solvents, ambient temperatures, and exposure to light irradiation on the stability of the AFB_1 solution CRMs were considered in this study according to ISO Guide 35.[36] The degradation products were analyzed, and the possible degradation pathways were proposed. The results revealed that the double bonds of the furan ring and the carbonyl and methoxy groups were the active sites for the degradation reactions of AFB_1. Moreover, the approach developed in this work is also applicable for the analysis and identification of the degradation products of AFB_1 in other matrices.

2. EXPERIMENTAL SECTION

2.1. Chemical Reagents and Solutions. Aflatoxin B_1 ($C_{17}H_{12}O_6$; 98.3 ± 1.0%) was obtained from the National Institute of Metrology (GBW10172, Beijing, China). Aflatoxin 8,9-diol (98%, AFB_1-diol, CAS: 196820-36-7) and aflatoxin P_1 (98%, AFP_1, CAS: 32215-02-4) were purchased from the First Standard Co., Ltd. (Tianjin, China). (Note: AFB_1 must be treated with extreme caution and care. The safety rules including wearing protective clothing, goggles, and gloves must be strictly followed through the whole experiment. The AFB_1 waste should be properly disposed of in a designated waste container with 5% hypochlorite solution. All sample vials and glassware used in the experiment were soaked in a 5% hypochlorite solution for 72 h prior to proper disposal.[37]) Acetonitrile (HPLC grade), methanol (HPLC grade), and ammonium acetate (HPLC-grade, purity >99.89%) were obtained from the Thermo Fisher Scientific Company (CA, USA). Water (HPLC grade) was obtained from Merck (Darmstadt, Germany). Chloroform (AR, with purity >99.5%) was purchased from the Beijing Institute of Chemical Reagents (Beijing, China). Acetonitrile, methanol, and chloroform were used as solvents to prepare the stock solutions of AFB_1, which were stored in bottles covered with foil paper and held at −20 °C in a refrigerator for subsequent usages.

2.2. Aging at Various Temperatures and Exposure to Light Irradiations. The acetonitrile solution of AFB_1 was

https://doi.org/10.1021/acsomega.2c05829
ACS Omega 2022, 7, 40548−40557

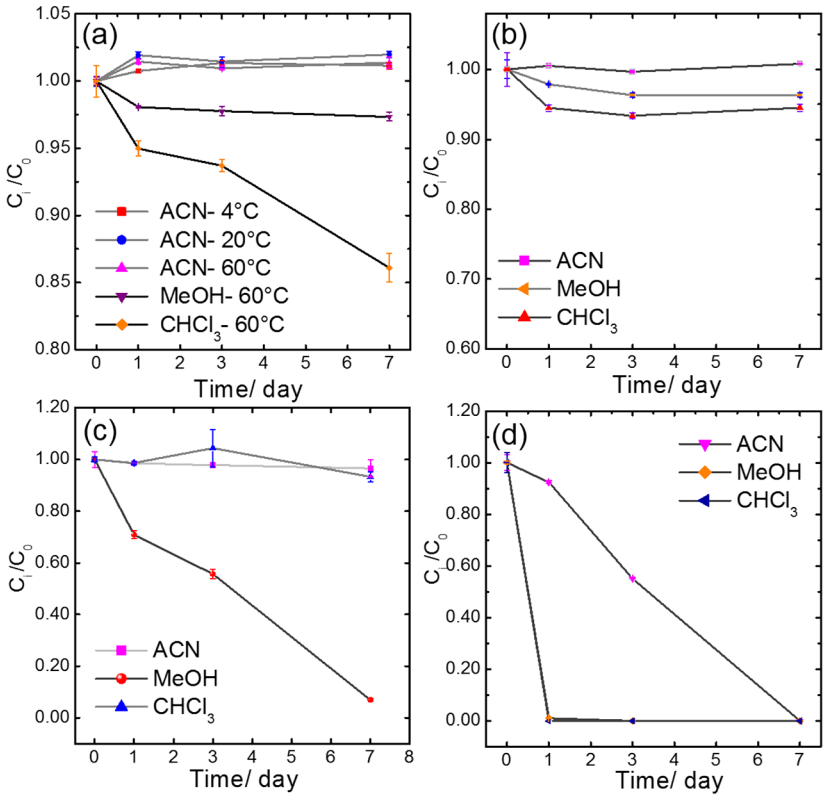

Figure 2. (a) Variation of the normalized AFB_1 fractions in various solvents at different temperatures (a) and in the cases of exposure to the fluorescent lamp (b), the sunlight (c), and the UV light with a wavelength of 360 nm (d).

held in the dark at 4, 20, and 60 °C, respectively, for 1, 3, 5, and 7 days and then analyzed with UHPLC coupled with Orbitrap MS. The same procedure was applied to the methanol and chloroform solutions except that these two solutions were held only at 60 °C. All three solutions were also exposed to different light irradiations when they were held at 20 ± 3 °C. The distance between the solutions and the light source was 90 cm in the experiments of exposure to the light irradiation from a fluorescent lamp and a UV light lamp (Spectroline, U.S.A., wavelength 360 nm), respectively. In the case of exposure to the sunlight, the solutions were illuminated by the sunlight directly. The experiments were performed in triplicate for each sample, and the samples were characterized on days 0, 1, 3, and 7. Five sample replicates were conducted for each experiment.

2.3. Characterizations with UHPLC-QE Plus Orbitrap MS. UHPLC characterization was performed on a Thermo Vanquish ultra-high performance liquid chromatography system (Thermo Fisher Scientific, U.S.A.) equipped with a DAD, an auto-injector, and a binary solvent delivery system. The DAD was set at 223, 263, and 360 nm. Chromatography separation was performed on a Thermo BDS HYPERSIL C18 column (250 × 4.6 mm, 5 μm, Thermo Fisher Scientific, U.S.A.). The column temperature was maintained at 27 °C. The injection volume was 2 μL, and the flow rate was 0.8 mL min^{-1}. The mobile phase was composed of 2 mM ammonium acetate aqueous solution (A) and acetonitrile (B). The gradient elution started with 10% B for 5 min and then increased linearly to 45% within 5 min, and the composition was kept for 3 min. For the following 5 min, another linear increased to 95% B and held for 3 min. Finally, B was switched to 10% B in 21.01 min and kept for 4 min before the next injection. The total operation time was 25 min.

Mass spectrometry was performed on a Thermo QE plus Orbitrap MS detection system with an electrospray ionization (ESI) source. The parameters were set as follows: spray voltages were +3.50 kV in positive mode and −3.00 kV in negative mode, the capillary temperature was 350 °C, the auxiliary gas heater temperature was 475 °C, sheath gas flow rate was 60 arbitrary units (arb.), auxiliary gas flow rate was 18 arb., sweep gas follow rate was 0 arb., and the S-lens RF level was 50.0 V. The data was acquired in full MS/data-dependent MS^2 ($dd\text{-}MS^2$) mode, which can provide an entire spectrum of fragment ion peaks for each degradation product. The full MS was scanned in the range of m/z 200−800 at a mass resolving power of 70,000 FWHM. The isolation window of the $dd\text{-}MS^2$ was set to 1.0 m/z with a resolution of 17,500 FWHM. The normalized collision energies (NCEs) were set at 30, 50, and 70. The automatic gain control (AGC) target (the number of ions to fill C-Trap) was set to 1.0×10^6 with a maximum injection time of 50 ms. The data was acquired and processed by Xcalibur4.1 software (Thermo Fisher Scientific, USA). The Xcalibur4.1 could provide the chromatograms of different samples and the accurate m/z of precursors and fragment ions. Additionally, it could provide possible molecular formulas with different elemental compositions and accurate double bond equivalent (DBE). Thus, the potential structures of the compounds were proposed. Next, the Mass Frontier 7.0 software was applied to simulate MS/MS patterns of the proposed structures. The simulated MS/MS patterns of fragment ions were then compared with the experimental ones. If the mass deviation was less than 5 ppm, then the

https://doi.org/10.1021/acsomega.2c05829
ACS Omega 2022, 7, 40548−40557

proposed fragment ion was considered to represent the real structure of the degradation product.[32,38]

2.4. Statistical Analysis. The AFB_1 fraction of various solutions at a certain moment was normalized by the initial value according to the following equation:

$$\theta = C_i/C_0 \quad (1)$$

where C_0 is the initial mass fraction of AFB_1 in each solution stored at −20 °C and C_i is the mass fraction of AFB_1 at a certain moment. The stability of the AFB_1 solutions was evaluated by analyzing the variation of θ under various conditions according to ISO Guide 35.[36] The basic model for stability evaluation can be expressed as the following (eq 2):[36]

$$Y = \beta_0 + \beta_1 X + \varepsilon \quad (2)$$

where β_0 and β_1 are the regression coefficients, ε denotes the random error component, X denotes time, and Y is the property value of the AFB_1 solutions. A small value of $|\beta_1|$ less than $t_{0.95,\,n-2} \times s(\beta_1)$ means that the property value under discussion is stable, where $t_{0.95,\,n-2}$ represents the value of t-distribution with the degree of freedom of $n - 2$ (n is the sample size) at a significance level of 0.95 and $s(\beta_1)$ is the standard deviation of β_1. Furthermore, the uncertainty (u) of the property value resulting from the instability can be calculated according to the following equation (eq 3):[36]

$$u = s(\beta_1) \times X \quad (3)$$

where X is the time elapsed since the initial property value of the sample was characterized.

2.5. Method Validation. The acetonitrile solutions with various known AFB_1 concentrations were prepared and analyzed by using UHPLC coupled with Orbitrap MS to validate the method of measuring the AFB_1 fractions in the solutions. A linear response of the instruments was observed in the AFB_1 concentration range from 0.35 to 500 ng/mL. The limit of detection (LOD), the limit of quantification (LOQ), and repeatability were also evaluated to validate the method. Five sample replicates were conducted for each experiment in the study.

3. RESULTS AND DISCUSSION

Generally, the solvents and environmental conditions affect the stability of solution CRMs.[31,39] The initial AFB_1 fraction was set to be 100 mg/L, the effects of the solvents, the storage temperatures, and the exposure to light irradiation on the stability of the AFB_1 fractions were evaluated in this study, and the results are presented below.

3.1. Effect of Temperature and Solvent. Shown in Figure 2a is the variation of the normalized AFB_1 fractions in the various solvents with time. The data corresponding to Figure 2a are summarized in Table S1. As indicated in Figure 2a and Table S1, the AFB_1 fraction of the acetonitrile solution hardly changed after the solution was held at the temperatures of 4, 20, and 60 °C for 1, 3, and 7 days. A similar phenomenon was observed for the methanol solution of AFB_1, which was held at 60 °C for 1, 3, and 7 days. A significant variation of AFB_1 fraction with time was observed for the chloroform solution held at 60 °C. The AFB_1 fraction decreased to 86% of the initial value after 7 days of storage. The linear regression analysis was made on these data according to ISO Guide 35, and the parameters derived from the analysis are presented in Table S2. The AFB_1 fractions of the acetonitrile and methanol solutions were considered stable at the investigated temperatures since $|\beta_1| < t_{0.95,\,n-2} \times s(\beta_1)$. In the case of the chloroform solution held at 60 °C, a value of $|\beta_1|$ greater than $t_{0.95,\,n-2} \times s(\beta_1)$ indicates that the AFB_1 fractions of the chloroform solution should be considered unstable. Additionally, the uncertainty (u) of the AFB_1 fraction resulting from its variation with time was also evaluated using eq 3 and normalized by the initial AFB_1 fraction. The normalized uncertainty results are given in Table S2. As shown in Table S2, the lowest uncertainty, 0.60%, was observed for the acetonitrile solution held at 4 °C while the maximum uncertainty, 3.4%, was observed for the chloroform solution held at 60 °C. This indicates that acetonitrile is the preferred solvent over methanol and chloroform to prepare AFB_1 solution CRMs, and a low storage temperature of 4 °C is beneficial for the stability of the AFB_1 solution CRMs.

3.2. Effect of Exposure to Light Irradiation. The acetonitrile, methanol, and chloroform solutions of AFB_1 were exposed to the irradiation of the fluorescent lamp (FL), the sunlight (SL), and the ultraviolet light with a wavelength of 360 nm (UV light @360 nm) for 1, 3, and 7 days at a temperature of 20 ± 3 °C, and the variation of the AFB_1 fraction of each solution with time is shown in Figure 2b–d. The data corresponding to Figure 2b–d are summarized in Table S3. As revealed in Figure 2b, the AFB_1 fractions of all three solutions only changed slightly when they were exposed to the light irradiation of the FL. A rapid decrease in the AFB_1 fraction was observed for the methanol solution exposed to the sunlight, while the acetonitrile and chloroform solution under the same conditions only showed a slight variation of AFB_1 fractions. The UV light with a wavelength of 360 nm was selected to be used in the stability evaluation of the AFB_1 solutions because the maximum absorption was observed at 360 nm for the acetonitrile solution of AFB_1, as shown in Figure S1. When exposed to UV light, all three solutions of AFB_1 exhibited a rapid decrease in the AFB_1 fraction. The AFB_1 fractions of the methanol and chloroform solutions decreased to (nearly) 0 within 1 day, while the corresponding value of the acetonitrile solution reached 0 within 7 days. The data presented in Table S3 were analyzed with the linear regression technique, and the results are given in Table S4. All solutions are considered stable under the light irradiation of the FL in terms of the criterion $|\beta_1| < t_{0.95,\,n-2} \times s(\beta_1)$, while they are unstable when exposed to UV light. The methanol solution of AFB_1 was very sensitive to exposure to sunlight, as shown in Figure 2c. The instability of the methanol solution was also confirmed by the statistical analysis (Table S4). It is worth noting that the acetonitrile and chloroform solutions are stable when exposed to sunlight. The uncertainties of the AFB_1 fractions of the solutions originating from the exposure to the light irradiation were evaluated, and the results are also presented in Table S4. A normalized uncertainty of 0.37% was observed for the AFB_1 fraction of the acetonitrile solution, which was exposed to the FL for 7 days. This implies that the exposure to the FL has little effect on the stability of the acetonitrile solution of AFB_1, but the exposure to the UV light irradiation should be avoided to prevent the solutions from degradation.

3.3. Degradation Products of AFB_1 Solutions Exposed to UV Light. The methanol and acetonitrile solutions of AFB_1 were analyzed by using the hyphenated instruments of UHPLC and QE plus Orbitrap MS after they were exposed to the UV light irradiation to identify the degradation

https://doi.org/10.1021/acsomega.2c05829
ACS Omega 2022, 7, 40548−40557

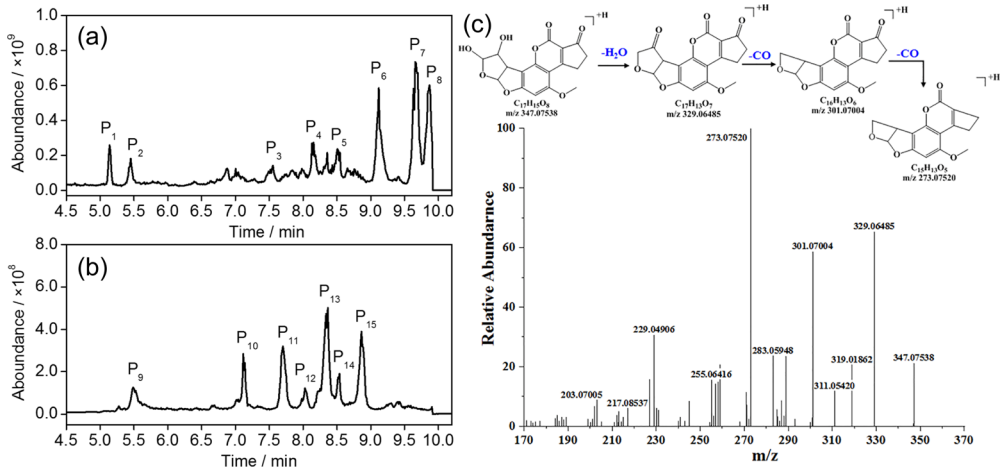

Figure 3. TIC of methanol (a) and acetonitrile (b) solutions of AFB_1 that were exposed to the UV light irradiation with a wavelength of 360 nm; (c) QE plus Orbitrap MS spectra and the proposed fragmentations of the degradation product (P_{10}) of the acetonitrile solution of AFB_1 exposed to the UV light irradiation.

Table 1. Mass of the Precursor Ions of the Degradation Products Measured Using UHPLC Coupled with QE Plus Orbitrap MS

			precursor ions		accuracy		
degradation products	RT (min)	molecular weight (Da)	experimental mass (m/z)	theoretical mass (m/z)	Δppm	molecular formula	DBE
P_1	5.14	332.05322	333.06009	333.06049	1.2	$C_{16}H_{12}O_8$	11
P_2	5.45	304.05830	305.06503	305.06560	1.9	$C_{15}H_{12}O_7$	10
P_3	7.55	362.10017	363.10785	363.10744	1.1	$C_{18}H_{18}O_8$	10
P_4	8.16	348.08452	349.09177	349.09179	0.06	$C_{17}H_{16}O_8$	10
P_5	8.51	316.05830	317.06537	317.06558	0.7	$C_{16}H_{12}O_7$	11
P_6	9.12	344.08960	345.09604	345.09688	−2.4	$C_{18}H_{16}O_7$	11
P_7	9.66	344.08960	345.09531	345.09688	−4.4	$C_{18}H_{16}O_7$	11
P_8	9.87	344.08960	345.09720	345.09688	0.09	$C_{18}H_{16}O_7$	11
P_9	5.50	274.04774	275.05466	275.05501	1.3	$C_{14}H_{10}O_6$	10
P_{10}	7.12	346.06887	347.07538	347.07614	−2.2	$C_{17}H_{14}O_8$	11
P_{11}	7.70	369.08485	370.09192	370.09213	−0.56	$C_{19}H_{15}NO_7$	13
P_{12}	8.06	332.05322	333.06049	333.06049	0	$C_{16}H_{12}O_8$	11
P_{13}	8.37	369.08485	370.09171	370.09213	−1.1	$C_{19}H_{15}NO_7$	13
P_{14}	8.48	330.03757	331.04440	331.04484	−1.3	$C_{16}H_{10}O_8$	12
P_{15}	8.86	298.04774	299.05432	299.05501	−2.3	$C_{16}H_{10}O_6$	12

products. The typical total ion chromatograms (TICs) of the degraded solutions are shown in Figure 3. Eight and seven peaks were observed in the TICs of the degraded methanol (Figure 3a) and acetonitrile (Figure 3b) solutions of AFB_1, respectively. The peaks and the corresponding degradation products are named P_1, P_2, P_3 ..., and P_{15}. TICs shown in Figure 3 also indicate that the degradation products were well separated by UHPLC. The precursor ions were acquired in the full MS mode in the study to identify the molecular formulas and chemical structures of the degradation products of AFB_1. The experimental mass values of precursor ions with high accuracy were measured and then analyzed with the Xcalibur4.1 software to deduce the possible molecular formula. The theoretical mass of each proposed molecular formula was compared with the as-obtained experimental value, and a proposed molecular formula was accepted if its theoretical mass agrees with the experimental value within 5 ppm.[32,38] The degradation product P_{11} was taken as an example to illustrate the process of determining the molecular formula. Three formulas, $C_{19}H_{16}O_7N$, $C_{16}H_{18}O_{10}$, and $C_{26}H_{12}O_2N$, were proposed for the precursor ion of P_{11}, and the deviations of the theoretical mass of each proposed formula from the experimental value were −0.56, 2.47, and 5.67 ppm, respectively. Another key parameter to estimate the molecular formula is the double bond equivalent (DBE) of the products, which should be close to that of AFB_1.[32] The DBE value of AFB_1 is 12, while the DBE values for $C_{19}H_{16}NO_7$, $C_{16}H_{18}O_{10}$, and $C_{26}H_{12}NO_2$ are 13, 8, and 21.5, respectively. Therefore, $C_{19}H_{16}NO_7$ was accepted as the correct formula since its DBE is the closest to that of AFB_1 and it has the least deviation from the experimental mass value. The retention time (RT), molecular weight, proposed molecular formula, mass error, and double bond equivalent (DBE) of the 15 degradation products are summarized in Table 1.

The data-dependent MS^2 (dd-MS^2) can provide the exact masses of the fragments.[38] Consequently, the dd-MS^2 was used to further elucidate the exact mass of the fragmental ions and the possible structures of the degradation products. Mass Frontier 7.0 was applied to simulate MS/MS patterns with mass deviations less than 5 ppm in the study, which enables the prediction of the most likely parental and fragmental structures of the degradation products. The corresponding MS/MS and fragmentations of the degradation compound P_{10} of the acetonitrile solution of AFB_1 are shown in Figure 3c.

https://doi.org/10.1021/acsomega.2c05829
ACS Omega 2022, 7, 40548−40557

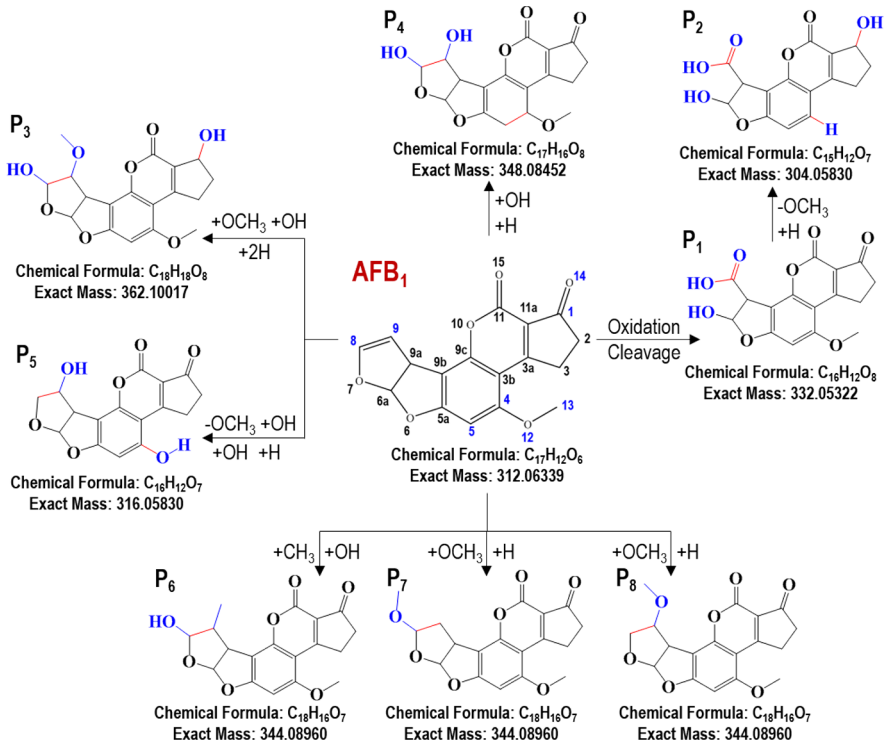

Figure 4. Degradation pathway of the methanol solution of AFB_1 exposed to the UV light irradiation with a wavelength of 360 nm.

The P_{10} yielded the precursor ion ($C_{17}H_{15}O_8$, $[M + H]^+$ at m/z 347.07538) peak, and several peaks of ionic fragments appeared at m/z 329.06485 [$C_{17}H_{13}O_7$, M-H_2O]$^+$, 301.07004 [$C_{16}H_{13}O_6$, M-H_2O-CO]$^+$, and 273.07520 [$C_{15}H_{13}O_5$, M-H_2O-CO-CO]$^+$. Based on these peaks, the P_{10} was considered to be formed *via* the addition of the −OH group on the furofuran ring of AFB_1.

Additionally, dd-MS^2 and fragmentations of the other 14 degradation products (P_1 to P_9 and P_{11} to P_{15}) are summarized in Figures S2−S15, respectively. The structures of the 15 degradation products were proposed based on the accurate mass values of the parent ions and fragments and are presented in Figure 1 with the corresponding IUPAC names listed in Table S5. The 15 degradation products maintained the chemical structures similar to AFB_1. The different parts in the structure were highlighted in colors. Obviously, the degradation processes were relevant to the slight modifications of the furofuran ring and cyclopentenone and methoxy groups in the structure of AFB_1 during the UV light irradiation.

3.4. Degradation Pathway of AFB_1 Solutions Exposed to UV Light. As discussed above, the methanol and acetonitrile solutions of AFB_1 exhibited different degradation behaviors at the exposure of UV light. The degradation pathway of the methanol solution of AFB_1 is presented in Figure 4. The degradation products are P_1 ($[M + H]^+$ at m/z 333.06009), P_2 ($[M + H]^+$ at m/z 305.06503), P_3 ($[M + H]^+$ at m/z 363.10785), P_4 ($[M + H]^+$ at m/z 349.09177), P_5 ($[M + H]^+$ at m/z 317.06537), P_6 ($[M + H]^+$ at m/z 345.09604), P_7 ($[M + H]^+$ at m/z 345.09531), and P_8 ($[M + H]^+$ at m/z 345.09720), which were confirmed by QE plus Orbitrap MS. The reactive species generated by the UV light irradiation have been considered to be responsible for the AFB_1 degradation. According to previous reports, the radiolysis of methanol could produce various chemical species, including methoxy species ($-OCH_3$), methyl species ($-CH_3$), hydroxyl species (−OH), and hydrogen species (−H).[40,41] These chemical species were considered to be initiators of the degradation of AFB_1. The degradation took place mainly *via* the addition reaction and oxidation reaction (Figure 4). In the first reaction path, the active species were added on the $C_8{=}C_9$ double bond of the furan ring of AFB_1. The P_6, P_7, and P_8 were the corresponding products of such addition reactions when the −OH, −H, $-OCH_3$, and $-CH_3$ groups reacted with the double bond ($C_8{=}C_9$).[42] Moreover, after the −OH group was added on the double bond ($C_8{=}C_9$) to form an intermediate product, the double bond ($C_4{=}C_5$) of the intermediate product could be further hydrogenated by −H species to produce the P_4.[43] When the −OH and $-OCH_3$ groups reacted with the double bond ($C_8{=}C_9$), followed by the hydrogenation of the carbonyl group ($C_1{=}O_{14}$), the degradation product P_3 was obtained.[33] When the hydration reaction takes place on the $C_8{=}C_9$ double bond, and the $-OCH_3$ group at the C_4 site was transformed to −OH, the degradation product P_5 was obtained.[28,32] The second reaction path mainly included epoxidation, oxidation, and addition reactions. The epoxidation of the double bond ($C_8{=}C_9$) of AFB_1 was the first step for the formation of degradation product P_1.[4] The epoxidation reaction was due to the hydroperoxyl radical ($HO_2^{\cdot}$) that was generated during the UV light exposure.[24] The epoxide group of the intermediate product was further cleaved and oxidized to form P_1.[4] Then, the $-OCH_3$ group at the C_4 site was cleaved and the carbonyl group at C_1 was hydrogenated to form the degradation product P_2.[24,44,45]

Nevertheless, as for the acetonitrile solution of AFB_1 exposed to the UV light irradiation, the degradation products are P_9 ($[M + H]^+$ at m/z 275.05466), P_{10} ($[M + H]^+$ at m/z 347.07538), P_{11} ($[M + H]^+$ at m/z 370.09192), P_{12} ($[M + H]^+$ at m/z 333.06049), P_{13} ($[M + H]^+$ at m/z 370.09171), P_{14} ($[M + H]^+$ at m/z 331.04440), and P_{15} ($[M + H]^+$ at m/z 299.05432). The degradation pathway of AFB_1 in acetonitrile

https://doi.org/10.1021/acsomega.2c05829
ACS Omega 2022, 7, 40548−40557

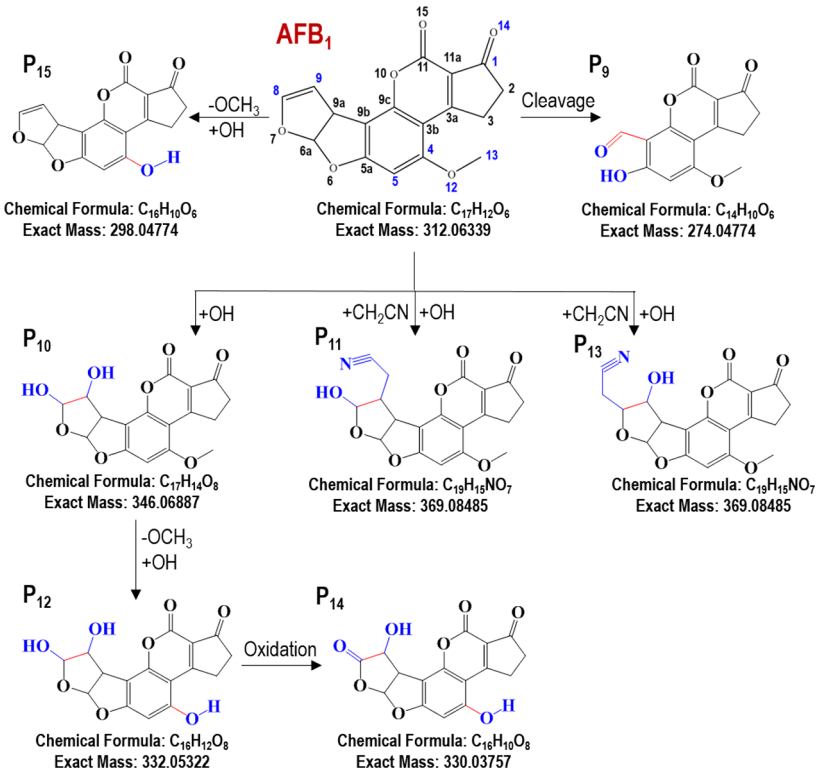

Figure 5. Degradation pathway of the acetonitrile solution of AFB_1 exposed to the UV light irradiation with a wavelength of 360 nm.

solution is shown in Figure 5. Similar to those in the methanol solution, the degradation processes in acetonitrile involved the addition and oxidization reactions. The photolysis of acetonitrile could lead to the formation of cyanomethyl species ($-CH_2CN$), cyano species ($-CN$), methyl species ($-CH_3$), and hydrogen species ($-H$).[46] Moreover, the photolysis of H_2O by the UV light can generate the hydroxyl species ($-OH$).[47] Consequently, it was supposed that $-CH_2CN$, $-OH$, $-H$, and $-CH_3$ radicals were the reactive species involved in the degradation process, which were generated in acetonitrile under the UV light irradiation. The addition of $-CH_2CN$ and $-OH$ groups on the double bond ($C_8{=}C_9$) of the furan ring of AFB_1 led to the formation of degradation products P_{10}, P_{11}, and P_{13}.[24,28,33,44,45,48] The $-OCH_3$ group at the C_4 site of P_{10} was cleaved and replaced by the hydroxyl species ($-OH$) to form the degradation product P_{12}. Further oxidation of P_{12} led to the formation of P_{14}. Moreover, the $-OCH_3$ group of AFB_1 could be cleaved, and then, the $-OH$ group was added to form the degradation product P_{15}.[4,45] Moreover, the furofuran ring of AFB_1 could be cleaved and further oxidized to produce degradation product P_9.[24,45] More importantly, among the degradation products, P_{10} and P_{15} were interpreted as aflatoxin B_1 8,9-dihydrodiol (AFB_1-diol) and aflatoxin P_1 (AFP_1), respectively. The commercially available AFB_1-diol and AFP_1 were analyzed by QE plus Orbitrap MS, and their spectra exhibited features closely similar to those of P_{10} and P_{15}, respectively, as shown in Figures S16 and S17, confirming the chemical structure of P_{10} and P_{15}, respectively.

According to the proposed degradation pathways of the methanol and acetonitrile solutions of AFB_1, the addition, epoxidation, hydration, and hydrogenation reactions of AFB_1 are responsible for the formation of various degradation products. In addition, the double bond, methoxy group, and carbonyl group ($C_8{=}C_9$, $C_4{=}C_5$, $C_1{=}O_{14}$, and $C_{13}{-}O_{12}$) of AFB_1 could act as the active sites during the degradation process when exposed to the UV light. The double bond ($C_8{=}C_9$) and methoxy group ($-OCH_3$) were active in both methanol and acetonitrile solutions. The above-mentioned reactions as well as active sites were also observed when plasma and ozone treatments were applied to AFB_1.[3,13,18,32] However, the other reaction sites, such as C_3 and C_{9a} in AFB_1, were efficiently activated only by microsomal enzymes, which resulted in the formation of other degradation products.[49,50] Thus, the degradation products and degradation pathways of the solutions of AFB_1 are dependent on the treatment techniques. Moreover, it was found that the degradation products and degradation pathways were also strongly related to the solvents to dissolve AFB_1. This provides new insight into the degradation behavior of the solution CRMs of AFB_1.

The method used in this study to characterize the degradation of the AFB_1 solutions was evaluated to validate its applicability. The linearity, limits of detection (LODs), limits of quantification (LOQs), and the precision of this method when it was applied in characterizing the AFB_1 solutions are summarized in Table S6. The data presented in Table S6 indicate that our method is reliable, accurate in the characterization of the degradation of the AFB_1 solutions.

4. CONCLUSIONS

In summary, the effects of the solvents, storage temperature, and exposure to light irradiation on the stability of the AFB_1 CRM solutions were evaluated for the first time. The results indicate that the stability of the AFB_1 solutions is dependent on the solvent, storage temperature, and light irradiation. UV light irradiation accelerates the degradation of AFB_1 in all solutions. The degradation products and degradation pathways of the methanol and acetonitrile solutions of AFB_1 were studied using ultra-high performance liquid chromatography

https://doi.org/10.1021/acsomega.2c05829
ACS Omega 2022, 7, 40548−40557

coupled with high-resolution mass spectrometry. The double bonds of the furan ring (C_8═C_9), carbonyl group, and methoxy group of AFB_1 were the reaction active sites in the degradation process. Different degradation behaviors were observed for the methanol and acetonitrile solutions of AFB_1. The possible degradation pathways were proposed based on the structures of the degradation products. The acetonitrile solution of AFB_1 can be very stable when it is stored at low temperatures, and the exposure to the UV irradiation is avoided. The findings of this study provide useful guides not only for the production, storage, and transportation of the solution CRMs of AFB_1 but also for the quantitative analysis of the possible impurities occurred in the solution CRMs of AFB_1.

■ ASSOCIATED CONTENT

Supporting Information

The Supporting Information is available free of charge at https://pubs.acs.org/doi/10.1021/acsomega.2c05829.

The normalized AFB_1 fractions and corresponding linear regression analysis at different temperatures; normalized AFB_1 fractions and corresponding linear regression exposed to the fluorescent lamp, sunlight, and UV light; IUPAC nomenclature of AFB_1 and the 15 degradation products; the linearity, LOD, LOQ, and repeatability of the method in the study; UV−vis absorption spectrum of AFB_1 CRM; various QE plus Orbitrap MS spectra and the proposed fragmentations of degradation products (P_1 to P_9 and P_{11} to P_{15}); comparison of the QE plus Orbitrap MS spectra (AFB_1-diol and P_{10}; AFP_1 and P_{15}) (PDF)

■ AUTHOR INFORMATION

Corresponding Authors

Xiaomin Li − *Food Safety Analysis Laboratory, Division of Chemical Metrology and Analytical Science, Key Laboratory of Chemical Metrology and Applications on Nutrition and Health for State Market Regulation, National Institute of Metrology, Beijing 100029, P. R. China*; Phone: +86-10-6452-4784; Email: lixm@nim.ac.cn; Fax: +86-10-6452-4737

Xiong Yin − *College of Chemistry, State Key Laboratory of Chemical Resource Engineering, Beijing University of Chemical Technology, Beijing 100029, P. R. China*; orcid.org/0000-0002-7109-2446; Phone: +86-10-6443-3197; Email: yinxiong@mail.buct.edu.cn; Fax: +86-10-6265-6765

Authors

Shuangqing Li − *Food Safety Analysis Laboratory, Division of Chemical Metrology and Analytical Science, Key Laboratory of Chemical Metrology and Applications on Nutrition and Health for State Market Regulation, National Institute of Metrology, Beijing 100029, P. R. China*

Xuehui Liu − *College of Chemistry, State Key Laboratory of Chemical Resource Engineering, Beijing University of Chemical Technology, Beijing 100029, P. R. China*

Qinghe Zhang − *Food Safety Analysis Laboratory, Division of Chemical Metrology and Analytical Science, Key Laboratory of Chemical Metrology and Applications on Nutrition and Health for State Market Regulation, National Institute of Metrology, Beijing 100029, P. R. China*; orcid.org/0000-0001-5166-8367

Jiaqi Fang − *College of Chemistry, State Key Laboratory of Chemical Resource Engineering, Beijing University of Chemical Technology, Beijing 100029, P. R. China*

Xiuqin Li − *Food Safety Analysis Laboratory, Division of Chemical Metrology and Analytical Science, Key Laboratory of Chemical Metrology and Applications on Nutrition and Health for State Market Regulation, National Institute of Metrology, Beijing 100029, P. R. China*

Complete contact information is available at: https://pubs.acs.org/10.1021/acsomega.2c05829

Notes

The authors declare no competing financial interest.

■ ACKNOWLEDGMENTS

The work was financially supported by the National Key Research and Development Program of China (no. 2016YFF0201106) and the Fundamental Research Funds for the Central Universities (buctrc202023).

■ REFERENCES

(1) Xue, Z.; Zhang, Y.; Yu, W.; Zhang, J.; Wang, J.; Wan, F.; Kim, Y.; Liu, Y.; Kou, X. Recent Advances in Aflatoxin B_1 Detection Based on Nanotechnology and Nanomaterials-A Review. *Anal. Chim. Acta* **2019**, *1069*, 1−27.

(2) Bräse, S.; Encinas, A.; Keck, J.; Nising, C. F. Chemistry and Biology of Mycotoxins and Related Fungal Metabolites. *Chem. Rev.* **2009**, *109*, 3903−3990.

(3) Xie, H.; Wang, X.; Zhang, L.; Wang, T.; Zhang, W.; Jiang, J.; Chang, P. K.; Chen, Z. Y.; Bhatnagar, D.; Zhang, Q.; Li, P. Monitoring Metabolite Production of Aflatoxin Biosynthesis by Orbitrap Fusion Mass Spectrometry and a D-Optimal Mixture Design Method. *Anal. Chem.* **2018**, *90*, 14331−14338.

(4) Diao, E.; Shan, C.; Hou, H.; Wang, S.; Li, M.; Dong, H. Structures of the Ozonolysis Products and Ozonolysis Pathway of Aflatoxin B_1 in Acetonitrile Solution. *J. Agric. Food Chem.* **2012**, *60*, 9364−9370.

(5) Ostry, V.; Malir, F.; Toman, J.; Grosse, Y. Mycotoxins as Human Carcinogens-the IARC Monographs Classification. *Mycotoxin Res.* **2017**, *33*, 65−73.

(6) Braun, D.; Ezekiel, C. N.; Abia, W. A.; Wisgrill, L.; Degen, G. H.; Turner, P. C.; Marko, D.; Warth, B. Monitoring Early Life Mycotoxin Exposures via LC-MS/MS Breast Milk Analysis. *Anal. Chem.* **2018**, *90*, 14569−14577.

(7) Albert, J.; More, C. A.; Dahlke, N. R. P.; Steinmetz, Z.; Schaumann, G. E.; Muñoz, K. Validation of a Simple and Reliable Method for the Determination of Aflatoxins in Soil and Food Matrices. *ACS Omega* **2021**, *6*, 18684−18693.

(8) Pires, N. A.; Oliveira, M. L. G. D.; Gonçalves, J. A.; Faria, A. F. Multiclass Analytical Method for Pesticide and Mycotoxin Analysis in Malt, Brewers' Spent Grain, and Beer: Development, Validation, and Application. *J. Agric. Food Chem.* **2021**, *69*, 4533−4541.

(9) Wu, X.; Zhang, X.; Yang, Y.; Liu, Y.; Chen, X. Development of a Deep Eutectic Solvent-Based Matrix Solid Phase Dispersion Methodology for the Determination of Aflatoxins in Crops. *Food Chem.* **2019**, *291*, 239−244.

(10) Turner, N. W.; Bramhmbhatt, H.; Szabo-Vezse, M.; Poma, A.; Coker, R.; Piletsky, S. A. Analytical Methods for Determination of Mycotoxins: an update (2009-2014). *Anal. Chim. Acta* **2015**, *901*, 12−33.

(11) *The State Food and Drug Administration of the National Health and Family Planning Commission of China*; National Standard of the People's Republic of China, GB2761−2017.

(12) Rodriguez, R. S.; O'Keefe, T. L.; Froehlich, C.; Lewis, R. E.; Sheldon, T. R.; Haynes, C. L. Sensing Food Contaminants: Advances in Analytical Methods and Techniques. *Anal. Chem.* **2021**, *93*, 23−40.
(13) Zhou, H.; Liu, N.; Yan, Z.; Yu, D.; Wang, L.; Wang, K.; Wei, X.; Wu, A. Development and Validation of the One-Step Purification Method Coupled to LC-MS/MS for Simultaneous Determination of Four Aflatoxins in Fermented Tea. *Food Chem.* **2021**, *354*, No. 129497.
(14) Oztekin, S.; Karbancioglu-Guler, F. Simultaneous Detection of Ochratoxin A and Aflatoxins in Industrial and Traditional Red and isot Pepper Flakes along with Dietary Exposure Risk Assessment. *ACS Omega* **2022**, 31756.
(15) Rausch, A. K.; Brockmeyer, R.; Schwerdtle, T. Development, validation, and application of a multi-method for the determination of mycotoxins, plant growth regulators, tropane alkaloids, and pesticides in cereals by two-dimensional liquid chromatography tandem mass spectrometry. *Anal. Bioanal. Chem.* **2021**, *413*, 3041−3054.
(16) Hidalgo-Ruiz, J. L.; Romero-González, R.; Martínez Vidal, J. L.; Frenich, A. G. A rapid method for the determination of mycotoxins in edible vegetable oils by ultra-high performance liquid chromatography-tandem mass spectrometry. *Food Chem.* **2019**, *288*, 22−28.
(17) Westwood, S.; Choteau, T.; Daireaux, A.; Josephs, R. D.; Wielgosz, R. I. Mass Balance Method for the SI Value Assignment of the Purity of Organic Compounds. *Anal. Chem.* **2013**, *85*, 3118−3126.
(18) Wise, S. A.; Phillips, M. M. Evolution of Reference Materials for the Determination of Organic Nutrients in Food and Dietary Supplements-a Critical Review. *Anal. Bioanal. Chem.* **2019**, *411*, 97−127.
(19) Ouakhssase, A.; Fatini, N.; Addi, E. A. Chemometric approach based on accuracy profile and data chronological distribution as a tool to detect performance degradation and improve the analytical quality control for aflatoxins' analysis in almonds using UPLC-MS/MS. *ACS Omega* **2021**, *6*, 12746−12754.
(20) Josephs, R. D.; Bedu, M.; Daireaux, A.; Li, X. Q.; Li, X. M.; Guo, Z.; Li, X. J.; Choteau, T.; Martos, G.; Westwood, S.; Wielgosz, R. I.; Li, H.; Simón, M.; Smersu, C. S.; Villarreal, M.; Seal, T. L.; Cirio, M.; Rego, E. C. P.; Leal, R.; Carvalho, L.; Rodrigues, J. M.; Guimarães, E.; Garrido, B. C.; Erazo, L. M.; Ramirez, S.; Gonzalez, I.; Giannikopoulou, P.; Alexopoulos, C.; Kakoulides, E.; Mugenya, I.; Prevoo-Franzsen, D.; Fernandes-Whaley, M.; Marbumrung, S.; Nammoonnoy, J.; Shearman, K.; Boonyakong, C.; Klich, H.; Torkhani, R.; Gokcen, T.; Bilsel, M.; Ozen, S. A.; Cea, J.; Martínez, O. Key comparison study - organic solvent calibration solution - gravimetric preparation and value assignment of aflatoxin B1 (AfB_1) in acetonitrile (ACN). *Metrologia* **2022**, *59*, No. 08002.
(21) Martos, G.; Westwood, S.; Josephs, R. D.; Choteau, T.; Li, X. M.; Guo, Z.; Wielgosz, R. I.*Calibrant Assessment Guideline: AfB1*, BIPM CAG-01, *Rapport BIPM-2019*/07 (2019) 1−30.
(22) Westwood, S.; Josephs, R. D.; Martos, G.; Choteau, T.; Li, X. Q.; Li, X. M.; Guo, Z.; Li, X. J.; Garrido, B., Un, I.*Purity Evaluation Guideline: AfB1*. BIPM PEG-02. Rapport BIPM-2021/01. 2021: 1−28.
(23) Josephs, R. D.; Li, X.; Li, X.; Guo, Z.; Garrido, B.; Un, I.; Daireaux, A.; Choteau, T.; Martos, G.; Westwood, S.; Li, H.; Wielgosz, R. I. The BIPM Mycotoxin Metrology Capacity Building and Knowledge Transfer Program: Accurate Characterization of a Pure Aflatoxin B1 Material to Avoid Calibration Errors. *J. AOAC Int.* **2019**, *102*, 1740−1748.
(24) Shi, H.; Cooper, B.; Stroshine, R. L.; Ileleji, K. E.; Keener, K. M. Structures of Degradation Products and Degradation Pathways of Aflatoxin B_1 by High-Voltage Atmospheric Cold Plasma (HVACP) Treatment. *J. Agric. Food Chem.* **2017**, *65*, 6222−6230.
(25) Guo, Y.; Zhao, L.; Ma, Q.; Ji, C. Novel Strategies for Degradation of Aflatoxins in Food and Feed: A Review. *Food Res. Int.* **2021**, *140*, No. 109878.
(26) Wang, R.; Liu, R.; Chang, M.; Jin, Q.; Huang, J.; Liu, Y.; Wang, X. Ultra-Performance Liquid Chromatography Quadrupole Time-of-Flight MS for Identification of Electron Beam from Accelerator Degradation Products of Aflatoxin B_1. *Appl. Biochem. Biotechnol.* **2015**, *175*, 1548−1556.
(27) Mir, S. A.; Dar, B. N.; Shah, M. A.; Sofi, S. A.; Hamdani, A. M.; Oliveira, C. A. F.; Moosavi, M. H.; Khaneghah, A. M.; Sant'Ana, A. S. Application of New Technologies in Decontamination of Mycotoxins in Cereal Grains: Challenges, and Perspectives. *Food Chem. Toxicol.* **2021**, *148*, No. 111976.
(28) Liu, R.; Wang, R.; Lu, J.; Chang, M.; Jin, Q.; Du, Z.; Wang, S.; Li, Q.; Wang, X. Degradation of AFB_1 in Aqueous Medium by Electron Beam Irradiation: Kinetics, *Pathway and Toxicology*. *Food Control* **2016**, *66*, 151−157.
(29) Marshall, H.; Meneely, J. P.; Quinn, B.; Zhao, Y.; Bourke, P.; Gilmore, B. F.; Zhang, G.; Elliott, C. T. Novel Decontamination Approaches and Their Potential Application for Post-Harvest Aflatoxin Control. *Trends Food Sci. Technol.* **2020**, *106*, 489−496.
(30) Yu, Y.; Shi, J.; Xie, B.; He, Y.; Qin, Y.; Wang, D.; Shi, H.; Ke, Y.; Sun, Q. Detoxification of Aflatoxin B1 in Corn by Chlorine Dioxide Gas. *Food Chem.* **2020**, *328*, No. 127121.
(31) Diaz, G. J.; Cepeda, S. M.; Martos, P. A. Stability of Aflatoxins in Solution. *J. AOAC Int.* **2012**, *95*, 1084−1088.
(32) Liu, R.; Jin, Q.; Tao, G.; Shan, L.; Huang, J.; Liu, Y.; Wang, X.; Mao, W.; Wang, S. Photodegradation Kinetics and Byproducts Identification of the Aflatoxin B1 in Aqueous Medium by Ultra-Performance Liquid Chromatography-Quadrupole Time-of-Flight Mass Spectrometry. *J. Mass Spectrom.* **2010**, *45*, 553−559.
(33) Wang, F.; Xie, F.; Xue, X.; Wang, Z.; Fan, B.; Ha, Y. Structure Elucidation and Toxicity Analyses of the Radiolytic Products of Aflatoxin B1 in Methanol-Water Solution. *J. Hazard. Mater.* **2011**, *192*, 1192−1202.
(34) Garcia, M.; Blanco, J. L.; Suarez, G. Aflatoxins B_1 and G_1 Solubility in Standard Solutions and Stability during Cold Storage. *Mycotoxin Res.* **1994**, *10*, 97−100.
(35) Johnson, W. W.; Harris, T. M.; Guengerich, F. P. Kinetics and Mechanism of Hydrolysis of Aflatoxin B_1 Exo-8,9-Epoxide and Rearrangement of the Dihydrodiol. *J. Am. Chem. Soc.* **1996**, *118*, 8213−8220.
(36) ISO Guide35. *Reference Materials-General and Statistical Principles for Certification*; ISO2006.
(37) Liao, C.-D.; Wong, J. W.; Zhang, K.; Yang, P.; Wittenberg, J. B.; Trucksess, M. W.; Hayward, D. G.; Lee, N. S.; Chang, J. S. Multi-mycotoxin Analysis of Finished Grain and Nut Products Using Ultrahigh-Performance Liquid Chromatography and Positive Electrospray Ionization−Quadrupole Orbital Ion Trap High-Resolution Mass Spectrometry. *J. Agric. Food Chem.* **2015**, *63*, 8314−8332.
(38) Dzuman, Z.; Zachariasova, M.; Veprikova, Z.; Godula, M.; Hajslova, J. Multi-analyte high performance liquid chromatography coupled to high resolution tandem mass spectrometry method for control of pesticide residues, mycotoxins, and pyrrolizidine alkaloids. *Anal. Chim. Acta* **2018**, *863*, 29−40.
(39) Li, X. Q.; Liu, S.; Guo, Z.; Li, X. M.; Jiao, H.; Zhang, Q. H. Stability of a calibrant as certified reference material for determination of trans-zearalenone by high performance liquid chromatography-diode array detection-triple quadrupole tandem mass spectrometry. *Anal. Bioanal. Chem.* **2022**, 3631.
(40) Kayanuma, M.; Shoji, M.; Furuya, K.; Aikawa, Y.; Umemura, M.; Shigeta, Y. Theoretical study of the photodissociation reaction of methanol. *Chem. Phys. Lett.* **2018**, *714*, 137−142.
(41) Öberg, K. I. Photochemistry and astrochemistry: photochemical pathways to interstellar complex organic molecules. *Chem. Rev.* **2016**, *116*, 9631−9663.
(42) Nakagawa, S. Relative Yields of Radicals Produced in Deuterated Methanol by Irradiation. *Radiat. Phys. Chem.* **2016**, *122*, 73−76.
(43) Iram, W.; Anjum, T.; Iqbal, M.; Ghaffar, A.; Abbas, M.; Khan, A. M. Structural Analysis and Biological Toxicity of Aflatoxins B1 and B2 Degradation Products Following Detoxification by Ocimum Basilicum and Cassia Fistula Aqueous Extracts. *Front. Microbiol.* **2016**, *7*, 1−18.

https://doi.org/10.1021/acsomega.2c05829
ACS Omega 2022, 7, 40548−40557

(44) Luo, X.; Wang, R.; Wang, L.; Wang, Y.; Chen, Z. Structure Elucidation and Toxicity Analyses of the Degradation Products of Aflatoxin B_1 by Aqueous Ozone. *Food Control.* **2013**, *31*, 331−336.
(45) Hojnik, N.; Modic, M.; Walsh, J. L.; Žigon, D.; Javornik, U.; Plavec, J.; Žegura, B.; Filipič, M.; Cvelbar, U. Unravelling the pathways of air plasma induced aflatoxin B1 degradation and detoxification. *J. Hazard. Mater.* **2021**, *403*, No. 123593.
(46) Svejda, P.; Volman, D. H. Photochemical Formation of Free Radicals from Acetonitrile as Studied by Electron Spin Resonance. *J. Phys. Chem.* **1970**, *74*, 1872−1875.
(47) Crosley, D. R.; Araps, C. J.; Doyle-Eisele, M.; McDonald, J. D. Gas-Phase Photolytic Production of Hydroxyl Radicals in an Ultraviolet Purifier for Air and Surfaces. *J. Air Waste Manage. Assoc.* **2017**, *67*, 231−240.
(48) Luo, X.; Wang, R.; Wang, L.; Li, Y.; Zheng, R.; Sun, X.; Wang, Y.; Chen, Z.; Tao, G. Analyses by UPLC Q-TOF MS of Products of Aflatoxin B1 after Ozone Treatment. *Food Addit. Contam. A.* **2014**, *31*, 105−110.
(49) Dhanasekaran, D.; Shanmugapriya, S.; Thajuddin, N.; Panneerselvam, A. Aflatoxins and aflatoxicosis in human and animals. *InTech.* **2011**, 221−254.
(50) Wu, Q.; Jezkova, A.; Yuan, Z.; Pavlikova, L.; Dohnal, V.; Kuca, K. Biological degradation of aflatoxins. *Drug Metab. Rev.* **2009**, *41*, 1−7.

https://doi.org/10.1021/acsomega.2c05829
ACS Omega 2022, 7, 40548−40557